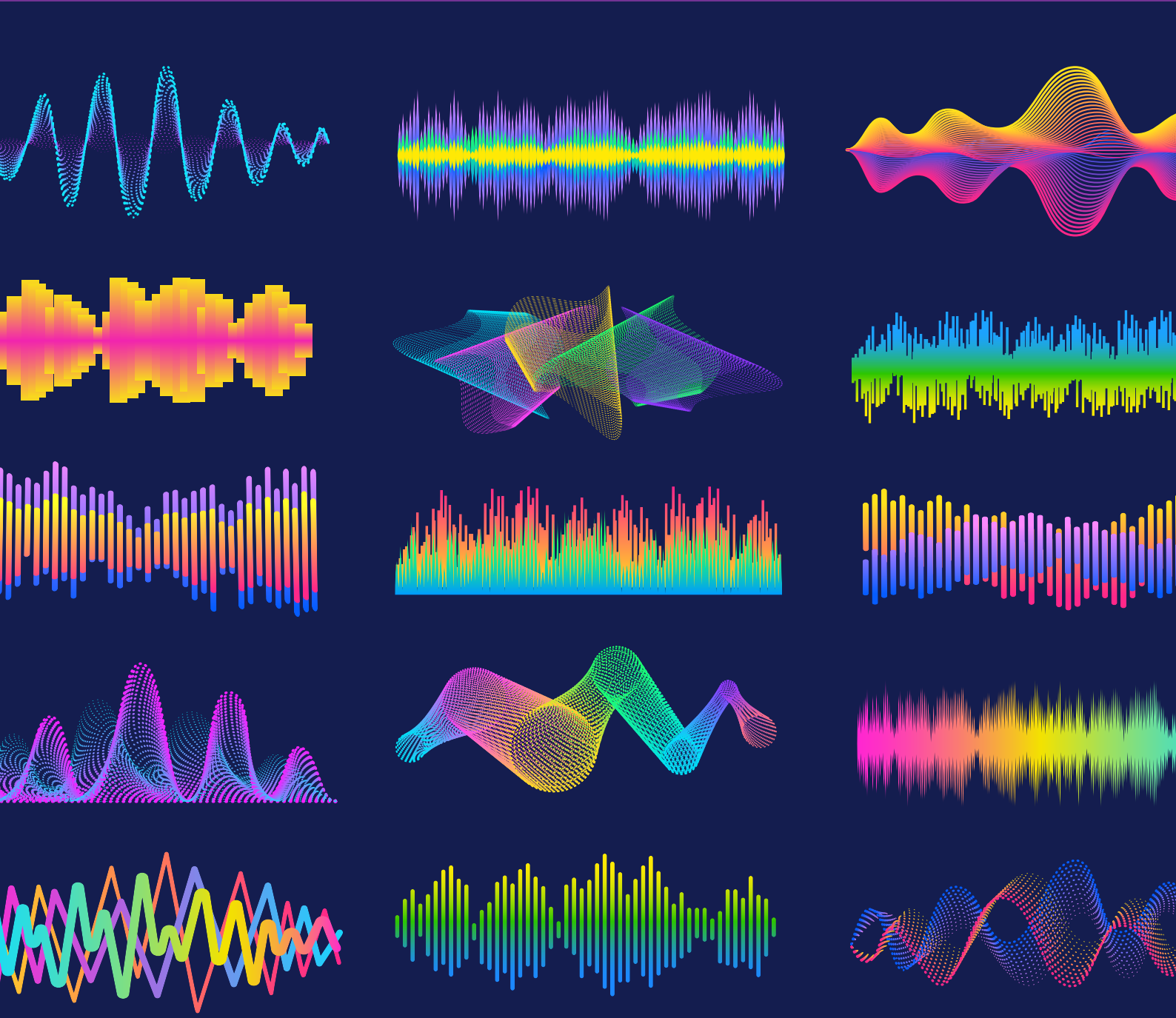


Portable Ultrasound System for Blood Velocity Estimation

Jeppe Hinrichs

Master Thesis



Portable Ultrasound System for Blood Velocity Estimation
Project Report

Master Thesis
April, 2023

Author:
Jeppe Hinrichs

Advisor(s):
Hyunjoo Lee, Associate Professor, School of Electrical Engineering, KAIST
Xenofon Fafoutis, Associate Professor, Department of Applied Mathematics and Computer Science, DTU
Tiberiu Gabriel Zsurzsán, Associate Professor, Department of Electrical Engineering, DTU

Copyright: Reproduction of this publication in whole, or in part, must include the customary bibliographic citation, including author attribution, report title, etc.

Cover photo: RawPixel, 2022

Published by (1): DTU, Department of Electrical Engineering, Ørsteds Plads, Building 348, 2800 Kgs. Lyngby, Denmark
www.elektro.dtu.dk

Published by (2): KAIST, , E3-2, 291 34141
www.ee.kaist.ac.kr

Timespan: Saturday 1st October, 2022 ~ Wednesday 12th April, 2023

Credits: 30 ECTS / 9 credits

Degree: Master of Science

Field: Electrical Engineering

Approval

This thesis has been prepared over six months at the Brain/Biomedical Microsystems Laboratory, School of Electrical Engineering, at the Korean Advanced Institute of Science and Technology, KAIST, and the Department of Electrical Engineering, Technical University of Denmark, DTU. This thesis is in partial fulfilment for the joint-degree Master of Science in Electrical Engineering, MSEE from KAIST and DTU.

Jeppe Hinrichs - s163555

.....
Signature

.....
Date

Contents

Preface	I
Contents	II
List of Figures	III
List of Tables	IV
Abbreviations	V
Glossary	VI
Reading comprehension	VII
1 Introduction	1
1.1 Project scope	2
2 Theory	5
2.1 Ultrasound	5
2.2 Flow physics	10
2.3 Devices	12
Bibliography	15
A Title	19

List of Figures

2.1	Particle displacement for a propagating ultrasound wave	5
2.2	Single element ultrasound transducer construction	8
2.3	Transducer types for acquiring B-mode images	9
2.4	Doppler effect diagram	10
2.5	Circulatory system of the human body	11
2.6	Diagram of ultrasound wave transmitted and reaching blood vessel with incident angle θ	12
2.7	Block diagram of continuous-wave flowmeter	13
2.8	Block diagram of pulsed-wave flowmeter	14

List of Tables

1.2	Comparison of medical imaging modalities	1
1.3	Project specification table	2
2.2	Approximate density, sound speed, and acoustic impedance of human tissue types	6
2.4	Approximate attenuation values for human tissue	7
2.6	Measured frequency shifts with a Doppler 3 MHz transducer at various velocities at a 45° incident angle	14

Abbreviations

Notation	Description
<i>CW</i>	continuous-wave
<i>PW</i>	pulsed-wave
<i>US</i>	ultrasound

Glossary

Notation	Description
adiabatic	Any process that happens without heat gain or loss is considered adiabatic
Doppler effect	A change in frequency of a wave in relation to an observer who is moving relative to the wave source
transcutaneous	Applied across the depth of the skin without invasive penetration

Reading comprehension

This section of the report will explain to the reader how to reference this document and explain the fundamental structure of the project as well as the report. Throughout the report, the reader will be assumed to be knowledgeable of basic circuit analysis and familiar with standard abbreviations typically used in electrical engineering. If not, readers can refer to the denotation section at the beginning of the report. It is assumed that the reader has a basic knowledge on the science of electrical engineering, physics, and circuit analysis.

Sources

Calculus expressions present in the report will typically have a reference explaining their origin. All references are prominently displayed with square brackets and a number, directing to the appendix in the last section of the report.

1 Introduction

The progress of diagnostic imaging has advanced significantly during the 20th century. As the cost of high speed computational systems has grown increasingly accessible, so has the use of medical imaging become prominent. Potentially millions of people have been spared painful exploratory surgery through non-invasive diagnostic imaging. And thus, lives can be saved by early diagnosis and intervention through medical imaging. Advancement in scientific visualization have in turn generated more complex datasets of increased size and quality. Four major technologies used are ultrasound (*US*), X-ray, computed tomography (*CT*), and magnetic resonance imaging (*MRI*). Each of the technologies have distinct advantages and disadvantages in biomedical imaging, thus each are still relevant for modern medicine. Table 1.2 contains a comparison and summary of the various fundamental diagnostic imaging modalities.

Modality	Ultrasound	X-ray	CT	MRI
Topic	Longitudinal, shear, mechanical properties	Mean X-ray tissue absorbtion	Local tissue X-ray absorbtion	Biochemistry (<i>T1</i> and <i>T2</i>)
Access	Small windows adequate	2 sides needed	Circumferential around body	Circumferential around body
Spatial resolution	Frequency and axially dependent, 0.2 mm to 3 mm	~ 1 mm	~ 1 mm	~ 1 mm
Penetration	Frequency dependent, 3 cm to 25 cm	Excellent	Excellent	Excellent
Safety	Excellent for > 50 years	Ionizing radiation	Ionizing radiation	Very good
Speed	Real-time	Minutes	20 minutes	Typical: 45 minutes, fastest: Real-time (<i>low-res</i>)
Cost	\$	\$	\$\$	\$\$\$
Portability	Excellent	Good	Poor	Poor
Volume coverage	Real-time volumes, proving	3D 2D	Large 3D volume	Large 3D volume
Contrast	Increasing (shear)	Limited	Limited	Slightly flexible
Intervention	Real-time 3D increasing	No, fluoroscopy limited	No	Yes, limited
Functional	Functional ultrasound	No	No	fMRI

Table 1.2: Comparison of medical imaging modalities [16]

Since medical imaging has been reportedly performed over 5 billion times as of 2004 [6], and later numbers from 2011 show a general doubling, and particularly a ten-fold increase in ultrasound examinations between year 2000 and 2011 [16]. Recent data reveals that this trend of doubling has continued through the years 2010 to 2020 [24], and reveals that even though patient processes were disrupted during the global SARS-CoV-2 pandemic, the number of medical imaging examinations per 1000 patients, still increased. The reasons for this, and particularly why ultrasound has been notably increased in use, can be attributed to its high, but inconsistent, resolution, cost effectiveness, portability, and real-time interventional imaging. The downside of ultrasound is its limited penetration and restrictions for use in certain body parts. When just comparing soft-tissue examinations, which ultrasound is limited to, both *CT* and *MRI* can image the entire body with consistent resolution and contrast, but are more expensive and has poor portability due to immense size of its hardware.

The cardiovascular system, which transports oxygen and nutrients to tissue, produces a complex flow pattern that cause velocity fluctuations. Several cardiovascular diseases are also known to cause abnormal blood flow. As mentioned earlier, ultrasound is a powerful tool for conducting non-invasive imaging of the cardiovascular system [12], [15], and has no adverse risk to patients. Determining power spectral density (*PSD*) of a received signal is a common way to estimate blood velocity. A processed image of the *PSD* over time is commonly known as a sonogram, where changes in blood velocity over time can be seen.

1.1 Project scope

The aim of this project is to study the application of ultrasound in the context of blood flow measurements. Various scientific articles have been studied to gain knowledge of prior research [3]–[5], [7]–[11], [13], [14], [18]–[23]. In addition, the textbooks [15]–[17] have also been instrumental in forming a solid knowledge base for the thesis. The desire is to build upon the vast knowledge already gathered by prominent researchers in the field of ultrasound systems for blood velocity estimation. Finally, using the knowledge gained, to design and implement an electronic device capable of performing these measurements using a novel approach. The project specifications are written in table 1.3.

Project specification

- Study and research ultrasound and its principles and applications
 - Design and implement a device for ultrasound blood velocity estimation
 - Investigate and test the device in an experimental setting
 - Validate results with commercial equipment
 - Make quantifiable performance measurements on system
 - Write a technical report documenting the project work
-

Table 1.3: Project specification table

The project is conducted under the guidance of advisors from the affiliated institutions Danmarks Tekniske Universitet (Technical University of Denmark) (*DTU*), Department of Electrical Engineering, Department of Applied Mathematics and Computer Science, and Korea Advanced Institute of Science and Technology (*KAIST*) at the Brain/Bio Medical Microsystems Laboratory.

The report is divided into five chapters, where the first part is an introduction to the project. The second chapter will focus on explaining the theory of the topic of the project.

The third chapter focuses on the synthesis of a system for experimental testing. The fourth chapter explains the production of the hardware. The fifth chapter will explain the testing methodology performed on the hardware. Finally, additional documentation of testing, code, circuit diagrams, and of laboratory setups can be found in the appendix.

2 Theory

2.1 Ultrasound

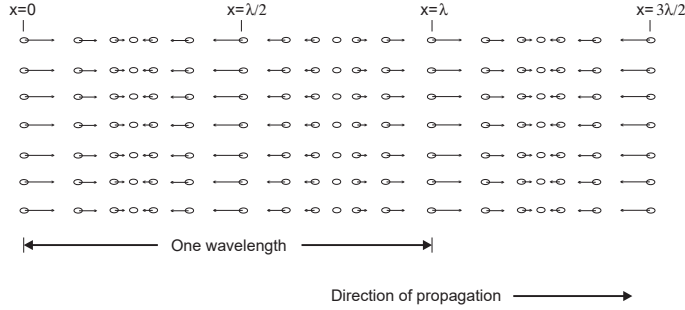


Figure 2.1: Particle displacement for a propagating ultrasound wave [15]

US is a technology that transmit sound wave with frequencies above the audible range (20 to 20 000 Hz) to mechanically vibrate matter. The particles in the medium would be at rest and distributed uniformly before any disturbance. The wave propagates as a disturbance and the particles oscillate around their mean position due to the presence of the ultrasonic wave. Typically the *US* frequency band used in clinical settings are from 1 to 15 MHz [16]. Figure 2.1 visualizes the propagation of a plane wave in matter. The oscillation occurs parallel to the wave's direction, making it longitudinal, and the disturbance will propagate with the variable c , which is determined by the medium and is given by eq. (2.1).

$$c = \sqrt{\frac{1}{\rho_0 \kappa_S}} \quad (2.1)$$

Where ρ_0 is the mean density (kgm^{-3}) and κ_S is the adiabatic compressibility (m^2N^{-1}). Since in the majority of cases, the propagation of ultrasound is linear, it is assumed in this work.

The acoustic pressure of the harmonic plane wave is expressed by eq. (2.2)

$$p(t, z) = p_0 e^{j(\omega t - kz)} \quad (2.2)$$

And propagates along the z -axis. ω is the angular frequency, k is the wave number and is expressed by $k = \omega/c = 2\pi/\lambda$, and p_0 is the acoustic pressure amplitude. A spherical wave is expressed by eq. (2.3)

$$p(t, r) = p_0 e^{j(\omega t - kr)} \quad (2.3)$$

Where r is radial distance, and is defined in a polar coordinate system. For each time instance, the acoustic pressure $p(t, r)$ is constant over a fixed radial position. In this scenario, the pressure amplitude is given by $p_0(r) = k_p/r$, where k_p is a constant since the energy of the outgoing wave must be constant. Particle speed u is dependent on the pressure caused by a wave expressed by eq. (2.4)

$$u = \frac{p}{Z} \quad (2.4)$$

Where Z is the characteristic acoustic impedance, defined as the ratio of acoustic pressure to particle speed at a given position in the medium and is expressed by eq. (2.5).

$$Z = \rho_0 c \quad (2.5)$$

Characteristic acoustic impedance Z is one of the most significant variables in the characterization of propagating plane waves. Reference values for density, speed of sound, and characteristic acoustic impedance can be seen in table 2.2.

Medium	Density (ρ_0) kg/m ³	Speed of sound (c) m/s	Characteristic acoustic impedance (Z) kg/(m ² s)
Air	1.2	333	0.4×10^3
Blood	1.06×10^3	1566	1.66×10^6
Bone	$1.38\text{--}1.81 \times 10^3$	2070–5350	$3.75\text{--}7.38 \times 10^6$
Brain	1.03×10^3	1505–1612	$1.55\text{--}1.66 \times 10^6$
Fat	0.92×10^3	1446	1.33×10^6
Kidney	1.04×10^3	1567	1.62×10^6
Lung	0.4×10^3	650	0.26×10^6
Liver	1.06×10^3	1566	1.66×10^6
Muscle	1.07×10^3	1542–1626	$1.65\text{--}1.74 \times 10^6$
Spleen	1.06×10^3	1566	1.66×10^6
Distilled water	1×10^3	1480	1.48×10^6

Table 2.2: Approximate density, sound speed, and acoustic impedance of human tissue types [15]

In the following sections, various acoustic wave phenomena will be briefly described.

2.1.1 Scattering

A wave propagating across a medium continues in the same direction until it encounters a new medium. When this occurs, a portion of the wave is transmitted into the new medium, with a change in direction. Because the scattered wave is the result of several contributors, it is necessary to define it statistically. The amplitude distribution is Gaussian [15] and can thus be fully described by its mean and variance. The mean value is zero because the dispersed signal is caused by variances of the acoustic characteristics in tissue.

The correlation between multiple data is what allows ultrasound to determine blood velocities. Because minor movements have a significant correlation, it is feasible to discover alterations in location by comparing sequential measurements of moving structure, such as blood cells. In medical ultrasound, just one transducer is utilised for transmitting and receiving, and only the backscattered signal is analysed.

The power of scattered signal is defined by the scattering cross-section, which in small cases mean a uniform intensity I_i , and is expressed by eq. (2.6).

$$P_s = I_i \sigma_{sc} \quad (2.6)$$

Where σ_{sc} is the scattering cross-section in square meters. The backscattering cross section is material dependant and determines the intensity of the scattering. If the dispersed

energy is evenly emitted in all directions, the scattered intensity is given by eq. (2.7).

$$I_s = \frac{P_s}{4\pi R^2} = \frac{\sigma_{sc}}{4\pi R^2} \cdot I_i \quad (2.7)$$

Where R is distance to the scattering region [15]. This results in a spherical wave. A transducer with radius r gives the power P_r , presuming the attenuation and focus is neglected, and is expressed by eq. (2.8).

$$P_r = I_s \pi r^2 = \sigma_{sc} \frac{r^2}{4R^2} \cdot I_i \quad (2.8)$$

The backscattering coefficient, which characterizes scattering from a volume of scatterers, is another measure of scattering strength. It is defined as average received power per steradian volume of scatterers when flooded with plane waves of unit amplitude and the unit is 1/cm³.

Back scattering coefficients in blood are significantly lower than the back scattering coefficients from various tissue types. This poses a challenge when estimating blood flow close to tissue vessel walls [2], [15].

2.1.2 Attenuation

The ultrasonic wave will be reduced as it propagates through tissue due to absorption and scattering. The attenuation in tissue is frequency dependent, with greater attenuation with increasing frequency. Because of absorption and dispersion, the ultrasonic wave will be attenuated as it travels through tissue. The relationship between attenuation, distance traveled, and frequency is frequently linear. Attenuation in tissue occurs as a result of both dispersion, which spreads energy in all directions, and absorption, which turns it to thermal energy.

Tissue	Attenuation dB/(MHz·cm)
Liver	0.6–0.9
Kidney	0.8–1
Spleen	0.5–1
Fat	1–2
Blood	0.17–0.24
Plasma	0.01
Bone	16–23

Table 2.4: Approximate attenuation values for human tissue [15]

The pressure of a wave propagating in Z -direction decreases exponentially expressed by eq. (2.9)

$$p(z) = p(z = 0)e^{-\alpha z} \quad (2.9)$$

Where $p(z = 0)$ is the pressure in the point of origin and α is the attenuation coefficient. The attenuation coefficient unit is Npcm⁻¹ and alternatively, dBcm⁻¹ with the relationship described in eq. (2.10).

$$\alpha = \frac{1}{z} \ln \frac{p(z=0)}{p(z)} \quad (2.10a)$$

$$\alpha(\text{dBcm}^{-1}) = 20(\log_{10}e)\alpha(\text{Npcm}^{-1}) = 8.68\alpha(\text{Npcm}^{-1}) \quad (2.10b)$$

The significance of absorption and scattering in ultrasonic attenuation in biological tissues is a point of contention. Scattering adds just a few percent to attenuation in most soft tissues. As a result, it is fair to conclude that absorption is the primary mechanism for ultrasonic attenuation in biological tissues [17].

2.1.3 Transducer

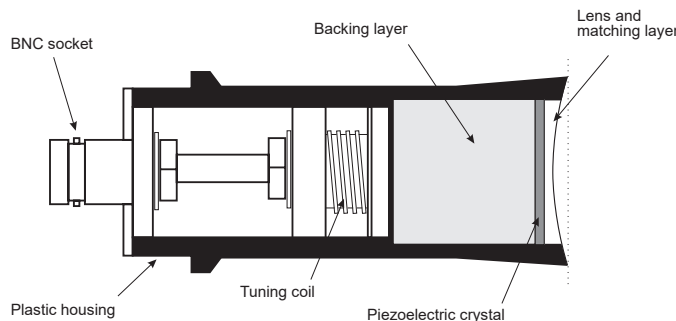


Figure 2.2: Single element ultrasound transducer construction [15]

A layperson knows transducers as speakers and microphones in the context of PA systems. In the case of medical *US* it is the device that generates the acoustic pressure field, which is emitted into tissue. The transducer has a piezoelectric crystal inside the housing. When excited, this crystal emits ultrasound waves toward flowing blood. The red blood cells will reflect a fraction of the emitted waves. These reflected waves are of a different frequency than the transmitted wave. If the red blood cells are moving away from the transducer, the frequency will be lower. If the red blood cells are moving towards the transducer, the frequency will be higher. This is caused by the Doppler effect. The reflected ultrasonic waves return to the crystal and are converted back into electrical signals. The single element transducer shown in fig. 2.2 has a minimal imaging window and has to be mechanically manipulated to get a wide window, which is unfeasible for responsive high-frequency imaging. Thus, usually an array transducer is used. Various *US* transducer types exist with different strengths and weaknesses, shown in fig. 2.3.

2.1.4 Doppler effect

The Doppler effect is a phenomena in which an observer perceives a shift in the frequency of sound emitted from a source when either the source or the observer is moving, or both are moving. The reason for the perceived change in frequency is visualised in fig. 2.4. In diagram (a), the source S_p is stationary and producing a spherical distribution pattern of the wave with the perceived frequency of the observer is given by $f = c/\lambda$, where c is the velocity of the wave in the medium and λ is the wavelength. In diagram (b), the sound source is moving towards the right with a velocity v . The locomotion of the source changes the distribution pattern and causes a longer wavelength on the left, indicating a lower perceived frequency, and a shorter wavelength on the right, indicating a higher perceived frequency, both denoted as λ' in the diagram.

In the case of the observer on the right side, the perceived frequency becomes eq. (2.11).

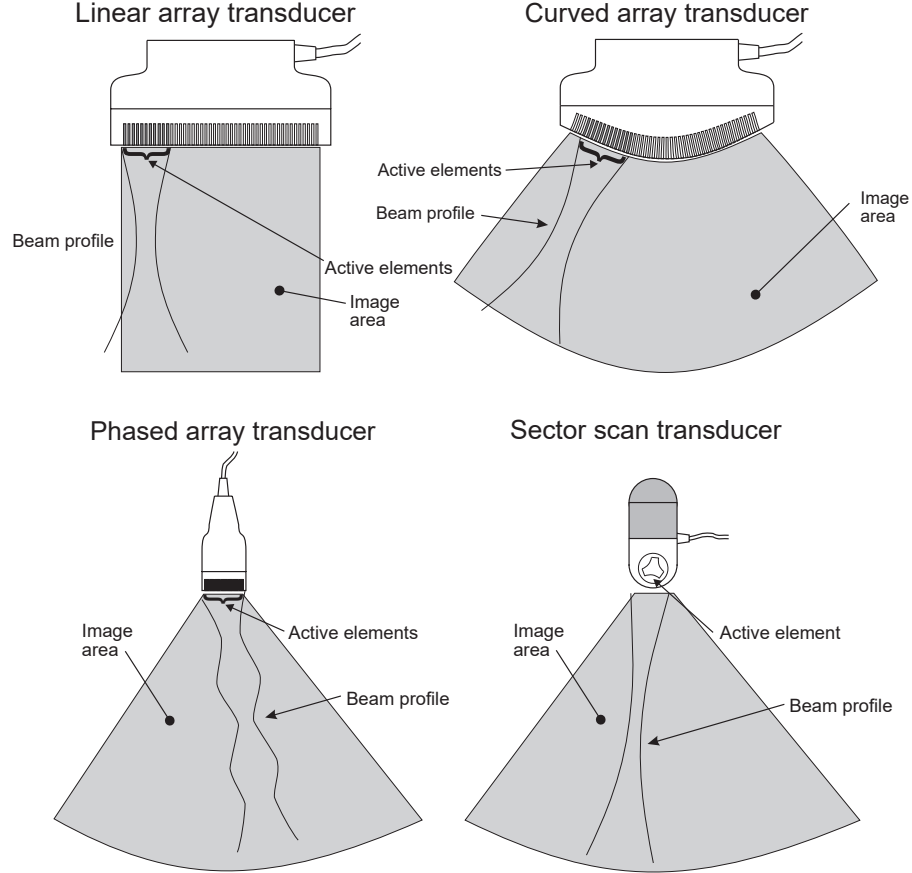


Figure 2.3: Transducer types for acquiring B-mode images [15]

$$f' = \frac{c}{\lambda} = \frac{c}{\lambda - vT} = \frac{c}{(c - v)T} = \frac{c}{c - v} \cdot f_0 \quad (2.11)$$

And viceversa, on the left side, the perceived frequency becomes eq. (2.12).

$$f' = \frac{c}{c + v} \cdot f_0 \quad (2.12)$$

Where

This perceived difference between the frequency that is transmitted from the source f_0 , and the perceived frequency f' is also called the Doppler frequency, f_d . When these connections are combined, the Doppler frequency for a source moving with velocity v and an observer traveling with velocity v' is given by eq. (2.13).

$$f_d = f' - f = \left(\frac{c + v'}{c - v} - 1 \right) \quad (2.13)$$

If both source and observer are moving with the same velocity, v , assuming $c \gg v$, the v cancels out and the expression is reduced to eq. (2.14).

$$f_d = \frac{2vf}{c} \quad (2.14)$$

If the velocity of the moving source is traveling with an incident angle θ , the v in eq. (2.14) is replaced with $v(\cos \theta)$. This results in the expression found in eq. (2.15) and forms the

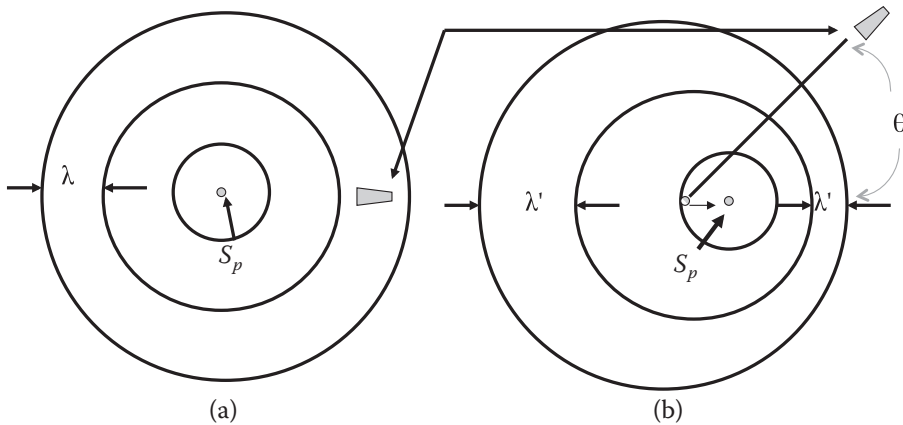


Figure 2.4: Doppler effect diagram. A stationary observer perceives a change in frequency of a wave generated by a moving source toward the observer as a result of a wavelength shift from λ to λ' . In (a), the source is still. In (b), the source is moving at a velocity v . [17]

basis for applied Doppler effect measurements.

$$f_d = \frac{2v(\cos \theta)f}{c} \quad (2.15)$$

The Doppler effect is utilised in ultrasonic Doppler devices used to image blood flow transcutaneously. An ultrasonic transducer in these devices sends ultrasonic waves into a blood artery, and the scattered radiation from moving red cells is measured by either the same transducer or a second transducer. The Doppler frequency, which is determined by the red blood cell velocity, is extracted using modern electronic demodulation techniques.

2.2 Flow physics

The flow physics of the human circulatory system are sophisticated and numerous non-stationary flow patterns emerge. The human circulatory system takes care of transporting oxygen and nutrients to the organs as well as disposing of waste products produced by metabolism. It is possible because the blood within the circulatory system contains several smaller subcomponents such as plasma and formed cellular elements that perform these vital functions. Initially, blood is discharged from the left ventricle of the heart via the aorta and travels to all areas of the body via multiple branches of the arterial tree. When the blood flows through the arteries, they into smaller channels known as arterioles. These arterioles lead into a network of tiny capillaries via which nutrients and waste materials are exchanged between the blood and the organs. The capillaries connect to form a network of venules, which supply the veins, which deliver blood back to the heart. This system, in its totality, is called the systemic circulation. A diagram of the circulatory system as described above, can be seen in fig. 2.5. In summary, when examining the elements that comprise the circulatory system, it consists of several components:

- Heart, primary organ of the circulatory system that maintains blood pressure and controls blood velocity.
- Blood, and its sub-components
 - Plasma, which forms the primary volume and contains nutrients and formed cellular elements.

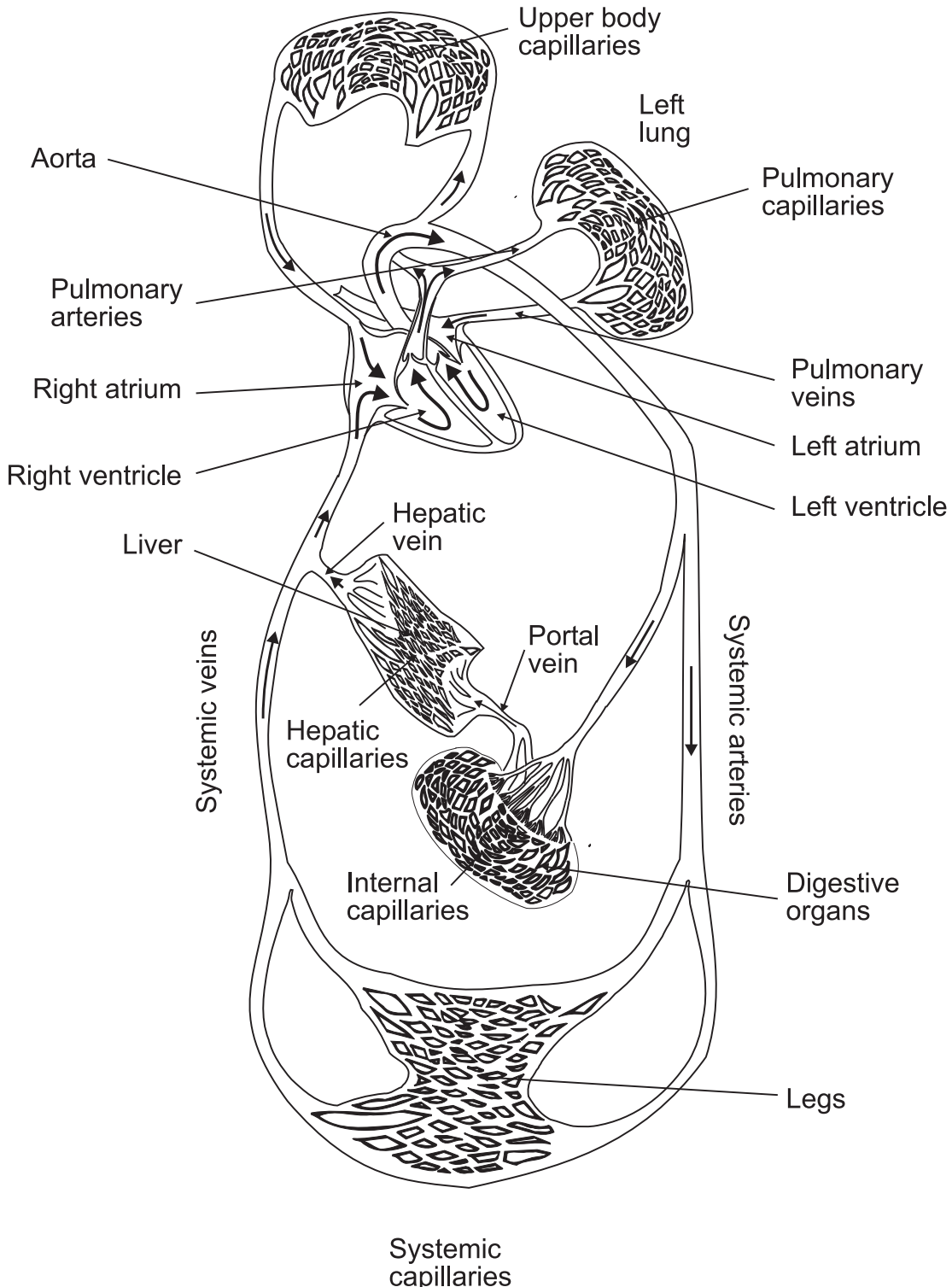


Figure 2.5: Circulatory system of the human body [15]

- Red and white blood cells, which carry oxygen and fight off infections, respectively.
- Platelets, which are also known as thrombocytes, with the function to clot during a blood vessel injury.

- Blood vessels
 - Arteries (and arterioles), that transport oxygenised blood to organs and tissues at high pressure and velocity.
 - Capillaries, thin but wide ranging blood vessels that performs the exchange of matter between the blood and tissues.
 - Veins (and venules), carries blood back to the heart at low pressure and velocity.

2.2.1 Blood flow

Blood flow, which is the amount of blood that goes through a blood vessel in a particular period of time, and has a complicated flow pattern due to its pulsing flow. An advanced analysis of haemodynamics is not within the scope of this report, so the explanation will be brief. The primary forces that determines the blood flow F are the pressure difference across a blood vessel and vascular resistance. It is determined by Ohm's law as in eq. (2.16).

$$F = \frac{\Delta P}{R} \quad (2.16)$$

Where ΔP is the pressure difference across the blood vessel and R is the vascular resistance. The pressure difference ΔP is calculated with eq. (2.17).

$$\Delta P = P_1 - P_2 \quad (2.17)$$

Where P_1 and P_2 are the blood pressures measured at each end of the blood vessel. Pressure has a significant importance on blood flow because an increase in arterial pressure not only increases the force that pushes blood through the capillaries, but it also expands the vessels, lowering vascular resistance.

2.3 Devices

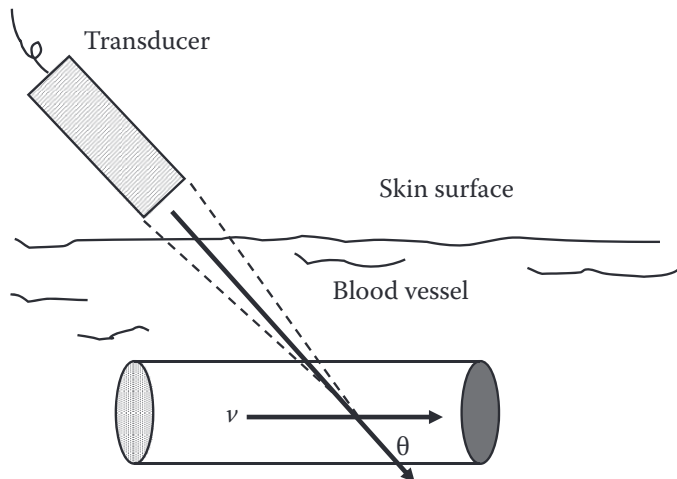


Figure 2.6: Diagram of *US* wave transmitted and reaching blood vessel with incident angle θ [17]

A device that measures the flowing of blood is called a flowmeter. Flowmeters may be used both inside and outside of vessels. One of the flowmeters that may be used outside the vessel to monitor flow is *US*. Figure 2.6 depicts an ultrasonic wave of frequency f insonifying a blood artery, resulting in an angle of θ relative to velocity v . For simplicity,

it is assumed that blood flows in a vessel at a constant velocity v . The echoes returned are shifted in frequency as described in eq. (2.15) in earlier in the chapter.

The echoes scattered by blood after being insonified by an ultrasonic wave convey information about the velocity of blood flow. Blood flow measurements are often used in clinical settings to determine the status of blood vessels and organ functioning. The two commonly used fundamental techniques for ultrasound Doppler flow measurements are continuous-wave (*CW*) and pulsed-wave (*PW*). Both will be explained.

2.3.1 Continuous-wave flowmeter

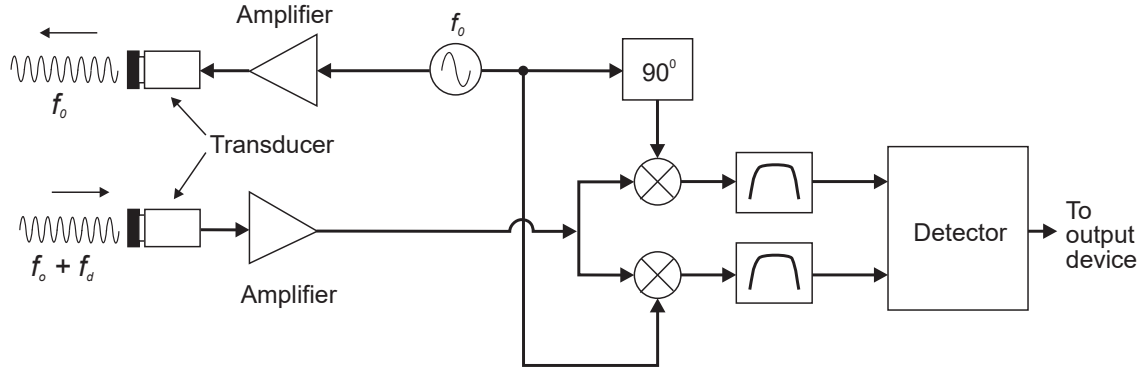


Figure 2.7: Block diagram of *CW* flowmeter [15]

The earliest non-invasive cardiovascular diagnostic technologies relied heavily on *CW* Doppler flowmeters. One of the earliest concepts for a device to estimate and study blood flow was proposed by Satomura, Yoshida, Mori, *et al.*[1] during the 1950's in Japan. To continuously transmit waves and receive signals from moving reflectors, the *CW* flowmeter uses two transducers. *CW* flowmeters use less sophisticated electronics than *PW* flowmeters. A drawback to the *CW* flowmeter is the lacking depth discrimination due to the continuous characteristic of this device type. A block diagram of a typical *CW* flowmeter can be seen in fig. 2.7.

The basic principles of the device is previously explained in the Doppler effect section, and the measurement of the device is described in eq. (2.11). The device continuously emits an ultrasonic wave in the first transducer expressed as a function of time by eq. (2.18) [15].

$$e(t) = \cos(2\pi f_0 t) \quad (2.18)$$

While receiving the backscattered signal on the second transducer expressed by eq. (2.19) [15].

$$r_s(t) = a \cos(2\pi f_0 \alpha(t - t_0)) \quad (2.19)$$

$$\alpha \approx 1 - \frac{2v_z}{c} \quad (2.20)$$

$$\alpha t_0 \approx \frac{2d_0}{c} \quad (2.21)$$

Where v_z indicates the velocity in the z direction. Applying the Fourier transform, the expression yields eq. (2.22).

$$r_s(t) \cdot e^{j2\pi f_0 t} \iff R_s(f - f_0) \quad (2.22)$$

Where $R_s(f - f_0)$ is the Fourier transform of $r_s(t)$. The received signal is then multiplied with a quadrature signal of frequency f_0 to find the Doppler frequency in eq. (2.23).

$$m(t) = a [\cos(2\pi f_0 t) + j \sin(2\pi f_0 t)] \cos(2\pi f_0 \alpha(t - t_0)) \quad (2.23)$$

$$\begin{aligned} &= \frac{a}{2} \left\{ \cos(2\pi f_0 [(1 - \alpha)t - \alpha t_0]) + \cos(2\pi f_0 [(1 - \alpha)t - \alpha t_0]) \right. \\ &\quad \left. + j \sin(2\pi f_0 [(1 - \alpha)t - \alpha t_0]) + j \sin(2\pi f_0 [(1 - \alpha)t - \alpha t_0]) \right\} \end{aligned} \quad (2.24)$$

As is general for quadrature demodulation, the resulting signal contains the frequency components of the sum and difference of the emitted and received signals' frequencies. Generally a gls bp filter is used on the demodulated signal to remove the high frequency summed signal at twice the frequency of f_0 . The filtered signal after the bp filter is expressed by eq. (2.25) and contains the Doppler shift of the emitted signal.

$$m_f(t) \approx \frac{a}{2} e^{(j2\pi f_0 \frac{2v_z}{c} t)} e^{(-j2\pi f_0 \alpha t_0)} \quad (2.25)$$

where the second exponential term is the delay proportional to the time between transmission and receiving of the signal.

Velocity (v) m/s	Doppler frequency (f_d) Hz
0.01	28
0.1	276
0.5	1377
1	2755
2	5510
5	13 770

Table 2.6: Measured frequency shifts with a Doppler 3 MHz transducer at various velocities at a 45° incident angle [15]

Seen in table 2.6 is an example of measured Doppler frequencies using a 3 MHz transducer using the method shown in fig. 2.6. Note that the frequencies measured are all within the audible range.

2.3.2 Pulsed-wave flowmeter

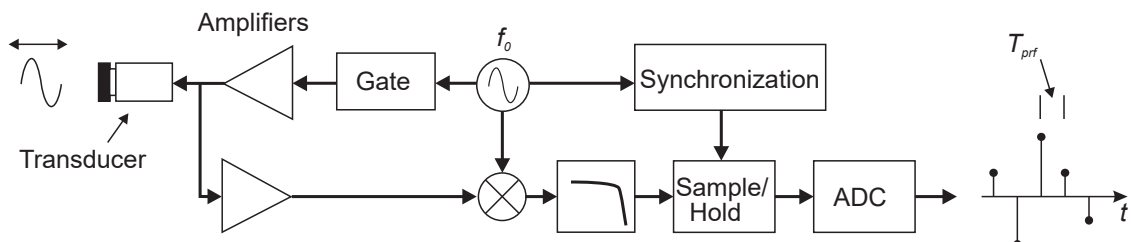


Figure 2.8: Block diagram of PW flowmeter [15]

Bibliography

- [1] S. Satomura, T. Yoshida, M. Mori, Y. Nimura, G.-i. Hikita, S. Takagishi, and K. Nakanishi, "Analysis of heart motion with ultrasonic Doppler method and its clinical application," *American Heart Journal*, vol. 61, pp. 61–75, 1 January 1961, ISSN: 00028703. DOI: 10.1016/0002-8703(61)90517-8. [Online]. Available: <https://linkinghub.elsevier.com/retrieve/pii/0002870361905178>.
- [2] K. K. Shung and G. A. Thieme, *Ultrasonic scattering in biological tissues*. CRC Press, 1993, p. 499, ISBN: 9780849365683. [Online]. Available: <https://www.routledge.com/Ultrasonic-Scattering-in-Biological-Tissues/Shung-Thieme/p/book/9780849365683>.
- [3] J. A. Jensen, "An Analysis of Pulsed Wave Ultrasound Systems for Blood Velocity Estimation," *Acoustical Imaging*, L. T. Piero and Masotti, Eds., pp. 377–384, 1996. DOI: 10.1007/978-1-4419-8772-3\61. [Online]. Available: <http://link.springer.com/10.1007/978-1-4419-8772-3%5C%5F61>.
- [4] P. J. Fish, "Ultrasonic investigation of blood flow," *Proceedings of the Institution of Mechanical Engineers, Part H: Journal of Engineering in Medicine*, vol. 213, pp. 169–180, 3 March 1999, Pmid: 10420772. DOI: 10.1243/0954411991534898. [Online]. Available: <https://doi.org/10.1243/0954411991534898>.
- [5] T. Jansson, H. W. Peresson, and K. Lindström, "Estimation of blood perfusion using ultrasound," *Proceedings of the Institution of Mechanical Engineers, Part H: Journal of Engineering in Medicine*, vol. 213, pp. 193–193, 3 March 1999, ISSN: 0954-4119. DOI: 10.1243/0954411991534915. [Online]. Available: <http://journals.sagepub.com/doi/10.1243/0954411991534915>.
- [6] E. Picano, "Sustainability of medical imaging," *Bmj*, vol. 328, pp. 578–580, 7439 March 2004, ISSN: 0959-8138. DOI: 10.1136/bmj.328.7439.578. [Online]. Available: <https://www.bmjjournals.org/lookup/doi/10.1136/bmj.328.7439.578>.
- [7] E. Chérin, R. Williams, A. Needles, G. Liu, C. White, A. S. Brown, Y.-Q. Zhou, and F. S. Foster, "Ultrahigh frame rate retrospective ultrasound microimaging and blood flow visualization in mice *in vivo*," *Ultrasound in Medicine & Biology*, vol. 32, pp. 683–691, 5 May 2006, ISSN: 03015629. DOI: 10.1016/j.ultrasmedbio.2005.12.015. [Online]. Available: <https://linkinghub.elsevier.com/retrieve/pii/S0301562906000172>.
- [8] X. Xu, J. Yen, and K. K. Shung, "A low-cost bipolar pulse generator for high-frequency ultrasound applications," *IEEE Transactions on Ultrasonics, Ferroelectrics and Frequency Control*, vol. 54, pp. 443–447, 2 February 2007, ISSN: 0885-3010. DOI: 10.1109/TUFFC.2007.259. [Online]. Available: <http://ieeexplore.ieee.org/document/4107704/>.
- [9] I. K. H. Tsang, B. Y. S. Yiu, D. K. H. Cheung, H. C. T. Chiu, C. C. P. Cheung, and A. C. H. Yu, "Design of a multi-channel pre-beamform data acquisition system for an ultrasound research scanner," *Ieee*, Sep. 2009, pp. 1840–1843, ISBN: 978-1-4244-4389-5. DOI: 10.1109/ULTSYM.2009.5441869. [Online]. Available: <http://ieeexplore.ieee.org/document/5441869/>.
- [10] E. A. Aydin and İ. Güler, "Design Of Pic-controlled Pulsed Ultrasonic Transmitter For Measuring Gingiva Thickness," *Instrumentation Science & Technology*, vol. 38, pp. 411–420, 6 October 2010, ISSN: 1073-9149. DOI: 10.1080/10739149.2010.509149. [Online]. Available: <http://www.tandfonline.com/doi/abs/10.1080/10739149.2010.509149>.

- [11] N. Matsuoka, D.-G. Paeng, R. Chen, H. Ameri, W. Abdallah, Q. Zhou, A. Fawzi, K. K. Shung, and M. Humayun, "Ultrasonic Doppler measurements of blood flow velocity of rabbit retinal vessels using a 45-MHz needle transducer," *Graefe's Archive for Clinical and Experimental Ophthalmology*, vol. 248, pp. 675–680, 5 2010, ISSN: 1435-702x. DOI: 10.1007/s00417-009-1298-9. [Online]. Available: <https://doi.org/10.1007/s00417-009-1298-9>.
- [12] K. L. Hansen, M. B. Nielsen, and J. A. Jensen, "In-vivo studies of new vector velocity and adaptive spectral estimators in medical ultrasound," 2011. [Online]. Available: <https://orbit.dtu.dk/en/publications/in-vivo-studies-of-new-vector-velocity-and-adaptive-spectral-estimator>.
- [13] C.-C. Huang, P.-Y. Lee, P.-Y. Chen, and T.-Y. Liu, "Design and implementation of a smartphone-based portable ultrasound pulsed-wave doppler device for blood flow measurement," *IEEE Transactions on Ultrasonics, Ferroelectrics and Frequency Control*, vol. 59, pp. 182–188, 1 January 2012, ISSN: 0885-3010. DOI: 10.1109/tuffc.2012.2171. [Online]. Available: <http://ieeexplore.ieee.org/document/6138742/>.
- [14] C. A. Winckler, P. R. Smith, D. M. J. Cowell, O. Olagunju, and S. Freear, "The design of a high speed receiver system for an ultrasound array research platform," Ieee, October 2012, pp. 1481–1484, ISBN: 978-1-4673-4562-0. DOI: 10.1109/ultsym.2012.0370. [Online]. Available: <http://ieeexplore.ieee.org/document/6562380/>.
- [15] J. A. Jensen, *Estimation of Blood Velocities Using Ultrasound: A Signal Processing Approach*, Third Edition. Department of Electrical Engineering, Technical University of Denmark, August 2013, ISBN: 9780521464840.
- [16] T. L. Szabo, *Diagnostic Ultrasound Imaging: Inside Out*, Second Edition. Elsevier, 2014, ISBN: 9780123964878. DOI: 10.1016/c2011-0-07261-7. [Online]. Available: <https://linkinghub.elsevier.com/retrieve/pii/C20110072617>.
- [17] K. K. Shung, *Diagnostic Ultrasound: Imaging and Blood Flow Measurements*, Second Edition. CRC Press, December 2015, ISBN: 978-1-4665-8264-4.
- [18] P. Govindan, B. Wang, P. Ravi, and J. Saniie, "Hardware and software architectures for computationally efficient three-dimensional ultrasonic data compression," *IET Circuits, Devices & Systems*, vol. 10, pp. 54–61, 1 January 2016, ISSN: 1751-858x. DOI: 10.1049/iet-cds.2015.0083. [Online]. Available: <https://onlinelibrary.wiley.com/doi/10.1049/iet-cds.2015.0083>.
- [19] B. Wang and J. Saniie, "Ultrasonic Signal Acquisition and Processing platform based on Zynq SoC," vol. 2016-August, Ieee, May 2016, pp. 0448–0451, ISBN: 978-1-4673-9985-2. DOI: 10.1109/eit.2016.7535282. [Online]. Available: <http://ieeexplore.ieee.org/document/7535282/>.
- [20] B. Wang and J. Saniie, "A High Performance Ultrasonic System for Flaw Detection," Ieee, October 2019, pp. 840–843, ISBN: 978-1-7281-4596-9. DOI: 10.1109/ultsym.2019.8926280. [Online]. Available: <https://ieeexplore.ieee.org/document/8926280/>.
- [21] H. Ding, D. Yang, J. Xu, X. Chen, X. Le, Y. Wang, L. Lin, and J. Xie, "Pulsed Wave Doppler Ultrasound Using 3.7 MHz Pmuts Toward Wearable Blood Flow Measurements," Ieee, January 2020, pp. 400–403, ISBN: 978-1-7281-3581-6. DOI: 10.1109/mems46641.2020.9056430. [Online]. Available: <https://ieeexplore.ieee.org/document/9056430/>.
- [22] B. Jana, R. Biswas, P. K. Nath, G. Saha, and S. Banerjee, "Smartphone-Based Point-of-Care System Using Continuous-Wave Portable Doppler," *IEEE Transactions on Instrumentation and Measurement*, vol. 69, pp. 8352–8361, 10 October 2020,

- ISSN: 0018-9456. DOI: 10.1109/tim.2020.2987654. [Online]. Available: <https://ieeexplore.ieee.org/document/9064842/>.
- [23] H. Ding, D. Yang, M. Qu, *et al.*, “A Pulsed Wave Doppler Ultrasound Blood Flowmeter by PMUTs,” *Journal of Microelectromechanical Systems*, vol. 30, pp. 680–682, 5 October 2021, ISSN: 1941-0158. DOI: 10.1109/jmems.2021.3103756. [Online]. Available: <https://ieeexplore.ieee.org/abstract/document/9515180>.
- [24] M. Winder, A. J. Owczarek, J. Chudek, J. Pilch-Kowalczyk, and J. Baron, “Are We Overdoing It? Changes in Diagnostic Imaging Workload during the Years 2010–2020 including the Impact of the SARS-CoV-2 Pandemic,” *Healthcare*, vol. 9, p. 1557, 11 November 2021, ISSN: 2227-9032. DOI: 10.3390/healthcare9111557. [Online]. Available: <https://www.mdpi.com/2227-9032/9/11/1557>.

A Title

Etiam lobortis facilisis sem. Nullam nec mi et neque pharetra sollicitudin. Praesent imperdier mi nec ante. Donec ullamcorper, felis non sodales commodo, lectus velit ultrices augue, a dignissim nibh lectus placerat pede. Vivamus nunc nunc, molestie ut, ultricies vel, semper in, velit. Ut porttitor. Praesent in sapien. Lorem ipsum dolor sit amet, consectetur adipiscing elit. Duis fringilla tristique neque. Sed interdum libero ut metus. Pellentesque placerat. Nam rutrum augue a leo. Morbi sed elit sit amet ante lobortis sollicitudin. Praesent blandit blandit mauris. Praesent lectus tellus, aliquet aliquam, luctus a, egestas a, turpis. Mauris lacinia lorem sit amet ipsum. Nunc quis urna dictum turpis accumsan semper.

DTU Electrical Engineering
Technical University
of Denmark

Ørsteds Plads, Building 348
2800 Kgs. Lyngby
Tel. (+45) 4525 3800

www.elektro.dtu.dk

KAIST EE
Korea Advanced Institute
of Science & Technology

E3-2, 291
34141
Tel. (+82) 042-350-2114

www.ee.kaist.ac.kr